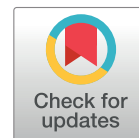


RESEARCH ARTICLE

Open Access



In silico molecular docking of luteolin as a potential antihyperpigmentation agent

Lucienne Agatha Larasati Nugraha Putri¹, Ni Luh Ari Krisma Anjani, Ni Putu Linda Laksmini^{1*}, Ni Made Pitri Susanti¹

Department of Pharmacy, Faculty of Mathematics and Natural Science, Udayana University, Bukit Jimbaran, Badung, Bali 80361, Indonesia

*Corresponding author: Bukit Jimbaran Campus, Udayana University, Badung, Bali 80361, Indonesia, Email: laksmini@unud.ac.id

Abstract: Excessive melanin synthesis, often triggered by overexposure to UV rays, is catalyzed by melanogenesis enzymes such as tyrosinase, tyrosinase-related protein 1, and D-dopachrome tautomerase. Derived from natural sources, the flavonoid compound luteolin is explored for its antihyperpigmentation potential. This study assesses luteolin's efficacy as an antihyperpigmentation agent by analyzing its affinity and bond interactions with melanogenesis enzymes through an *in silico* approach. Molecular docking, facilitated by HyperChem 8 for test compound optimization and Chimera 1.11.1 for protein preparation, alongside method validation and docking with AutoDockTools 1.5.6, established the protocol's validity with an RMSD value of ≤ 3 Å. Docking results reveal luteolin's higher affinity for the target proteins compared to native ligands, with binding energies of -5.63 kcal/mol for tyrosinase, -6.18 kcal/mol for tyrosinase-related protein 1, and -6.54 kcal/mol for D-dopachrome tautomerase. The interaction between luteolin and these proteins involves hydrogen, hydrophobic, electrostatic, and Van der Waals bonds, with amino acid residues His61, Lys129, Arg132 (tyrosinase); His192, His224, Val89 (tyrosinase-related protein 1); and Ile64, Asn73 (D-dopachrome tautomerase) participating in hydrogen bond formation. These findings suggest luteolin's significant potential as an antihyperpigmentation agent by inhibiting melanogenesis enzymes.

Keywords: antihyperpigmentation, hyperpigmentation, luteolin, *in silico*, molecular docking

Introduction

Skin serves as the body's primary defense against environmental factors. It is particularly susceptible to ultraviolet (UV) radiation, which, if exposure is excessive, can lead to uneven skin color, dryness, and the appearance of blackish-brown patches [1]. Hyperpigmentation, characterized by increased melanin production resulting in skin darkening, is more prevalent in Asia (21%) compared to other continents [2]. In Indonesia, the high incidence of hyperpigmentation is attributed to the predominance of skin types IV and V in the Fitzpatrick scale, which are less prone to burning but more likely to darken quickly [3]. This condition is exacerbated by Indonesia's tropical climate and intense sun exposure.

Increased local melanin synthesis or uneven distribution can cause localized pigmentation or dark spots on specific skin areas. Contributing factors include hormonal changes, inflammation, injury, acne, eczema, certain medications, and UV exposure [4]. Antihyperpigmentation agents work by inhibiting melanin synthesis [5], a process catalyzed by enzymes

such as tyrosinase, D-dopachrome tautomerase, and tyrosinase-related protein 1. Additionally, compounds with antioxidant activity, by inhibiting reactive oxygen species (ROS), can indirectly prevent hyperpigmentation. UV light, particularly in the dermis layer, can generate ROS, triggering melanogenesis through lipid peroxidation of melanocyte membranes [6].

Flavonoids are noted for their strong antioxidant activity [7]. Legundi leaves (*Vitex trifolia*), rich in flavonoids including luteolin (Figure 1), have been identified for their high antioxidant potential. Research indicates that luteolin can inhibit melanin synthesis in cells by targeting the tyrosinase enzyme [8]. However, literature reviews suggest that the specific potential of luteolin as an antihyperpigmentation agent, through the inhibition of melanogenesis enzymes, has yet to be reported. Thus, preliminary tests using molecular docking methods are necessary to ascertain luteolin's effectiveness as a melanogenesis enzyme inhibitor. Molecular docking can predict interactions between proteins and compounds, providing affinity values and interaction models crucial for determining luteolin's potential as an antihyperpigmentation agent.

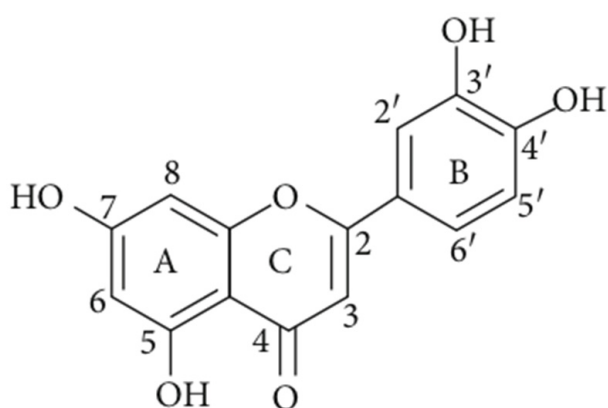


Figure 1. Chemical structure of luteolin

Methods

Three-dimensional structure optimization of test compound

The 3-dimensional structure of luteolin in simple data format (SDF) was obtained from the PubChem server (<https://pubchem.ncbi.nlm.nih.gov>). Then, the structure was converted using Protein Data Bank (PDB) using Open Babel Gui and optimized using the HyperChem8 program. The structural optimization used the Austin Model (AM1) semi-empirical computational method with single-point calculation and geometry optimization.

Protein target preparation

The target protein structures were obtained from <http://www.rcsb.org/pdb/home/home.do> and selected based on their structures in the active form bound to the native ligand. The protein targets used tyrosinase (PDB ID: 2Y9X), tyrosinase-related protein 1 (PDB ID: 5M8M), and D-dopachrome tautomerase (PDB ID: 3KAN). The preparation of the target protein was conducted using the Chimera 1.11.1 program.

Validation of molecular docking method

The molecular docking method was validated using AutoDock Tools 1.5.6, which was equipped with AutoDock4 and AutoGrid4 programs. The method validation involved redocking the native ligand of each target protein onto the target protein after removing its native ligand. The validation parameter for the molecular docking method was a Root Mean Square Deviation (RMSD) value ≤ 3.0 Å, indicating an acceptable protocol and allowing the docking of test compounds onto the target protein [9].

Docking of luteolin on target proteins

The optimized structure of luteolin was subjected to docking into a protein target from which the native ligand of the protein target had been removed. This process was carried out using AutoDockTools 1.5.6 application equipped with AutoDock4 and AutoGrid4 programs, employing a validated method. The docking results include binding energy values and the types of hydrogen bonds formed between the test compounds and the target proteins. Subsequently, data analysis was performed through a visualization process.

Data analysis

The analysis of the data employed descriptive methods. Findings obtained from molecular docking included information about binding energy and the type of bond formed between the compound (luteolin) and the protein target (tyrosinase, tyrosinase-related protein 1, and D-dopachrome tautomerase). The energy value indicates the affinity between the compound and the protein target. A more negative energy value signifies a stronger binding affinity of the ligand to the protein target.

Results

Three-dimensional structure optimization of test compound

Optimizing the 3-dimensional structure of the test compound includes single-point calculation and geometry optimization. The structure of the single-point calculation results and the optimization geometry of the test compound are shown in Table 1. Compared to the single-point calculation results, the test compound's geometry optimization results (luteolin) show lower total energy. The optimization of the luteolin 3D structure effectively reduces the overall energy during the optimization process. This leads to a stable structure with lower energy than the initial energy in single-point calculations.

Protein target preparation

Preparation was conducted on the 3D structure of target proteins (tyrosinase, tyrosinase-related protein 1, and d-dopachrome tautomerase). The preparation aims to separate the protein structure from the native ligand. Protein targets preparation were carried out on the 3D structure of the protein targets, namely tyrosinase (PDB ID: 2Y9X), tyrosinase-related protein 1 (PDB ID: 5M8M), and D-dopachrome tautomerase (PDB ID: 3KAN) which were obtained from <http://www.rcsb.org/pdb/home/home.do>.

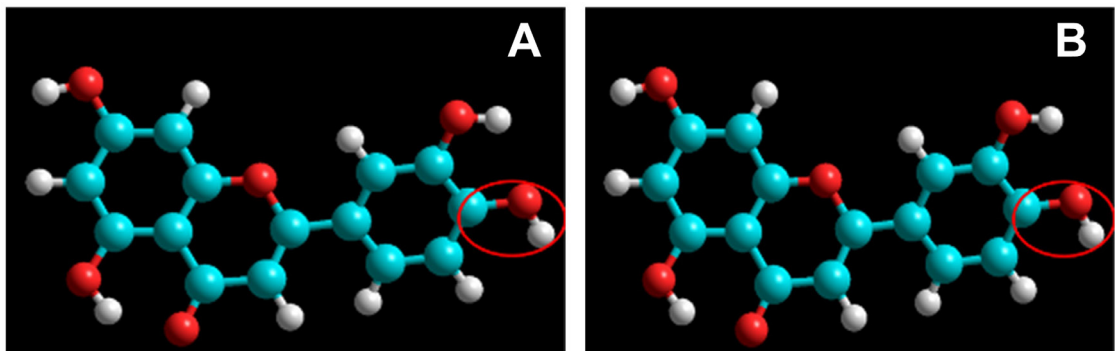


Figure 2. Optimization of luteolin structure. (A) Single point luteolin conformation, (B) Geometric optimization. The red circle shows the changes in the conformation of luteolin after geometric optimization

Table 1. Single point calculation results and optimization of test compound geometry

Compound	Total molecular energy (kcal/mol)	
	Single-point calculation	Geometry optimization
Luteolin	-3606.99	-3614.88

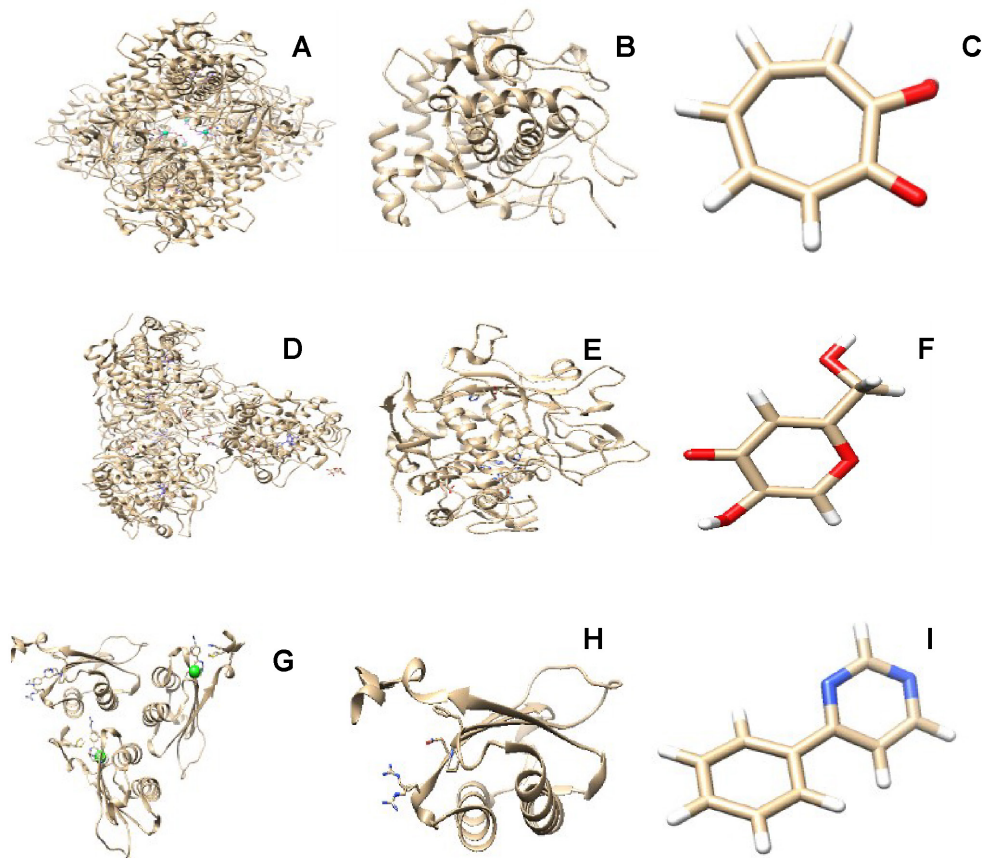


Figure 3. Target protein chain structure and native ligand. (A) Tyrosinase protein, (B) B chain tyrosinase without native ligand, (C) native ligand OTR, (D) Tyrosinase related protein 1, (E) Tyrosinase linked protein A chain 1, (F) native ligand KOJ, (G) D-dopachrome tautomerase protein, (H) chain C D-dopachrome tautomerase, (I) native ligand RW1; color in native ligand, red = O atom; blue = N atom

Table 2. The grid box setting on the target protein

Target proteins	Grid box		RMSD (Å)
	Grid size	Grid center	
Tyrosinase (PDB ID: 2Y9X)	x = 50 y = 50 z = 54	x = 2.798 y = 7.111 z = -8.073	0.99
Tyrosinase related protein 1 (PDB ID: 5M8M)	x = 70 y = 50 z = 60	x = -11.972 y = 3.361 z = -7.806	2.25
D-dopachrome tautomerase (PDB ID: 3KAN)	x = 60 y = 60 z = 60	x = 2.472 y = -6.222 z = 1.361	2.42

Table 3. Docking results between target protein and test compound

Protein target	Ligand	Bond energy (kcal/mol)	Amino acid residue	Group in hydrogen bonds (protein-ligand)
Tyrosinase (2Y9X)	Native ligand	-4,92	His61	HE2-OA2
	Luteolin	-5,63	Lys129 Arg132	HZ2-O HH22-O
Tyrosinase related protein 1 (5M8M)	Native ligand	-5,15	His192 His224	HE2-O6 HE2-O6
	Luteolin	-6,18	Val89	HN-O
D-dopachrome tautomerase (3KAN)	Native ligand	-6,46	Ile64	HN-N3
	Luteolin	-6,54	Asn73	HD21-O

Note:

The number after the amino acid residue indicates its sequence within protein's amino acid chain; Example: His61 (61st order histidine amino acid residue); His (histidine); Lys (lysine); Arg (arginine); Val (valine); Ile (isoleucine); Asn (asparagine); HE2-OA2 (Hydrogen atom (H) position E (epsilon) number 2 on the amino acid residue binds to the oxygen atom position A2 on ligand); HZ2-O (Hydrogen atom position Z (zeta) number 2 on the amino acid residue binds to the oxygen atom in on ligand).

Validation of molecular docking method

From the ten conformations of the native ligand within the binding site of the protein target, the most favorable conformation characterized by the lowest RMSD value was chosen. This specific conformation was selected due to its adherence to the RMSD requirement of ≤ 3 Å, indicating a close alignment of the native ligand's coordinates with its initial position within the active site of the protein target [9].

Docking of luteolin on target protein

The docking process for the luteolin resulted in ten conformations showing interaction with each target protein: tyrosinase, tyrosinase-related protein 1, and D-dopachrome tautomerase. Table 3 presents the values of the most negative bond energies and the hydrogen bonds formed through docking in the selected conformation of luteolin with their respective target proteins tyrosinase, tyrosinase-related protein 1, and D-dopachrome tautomerase.

Discussion

Luteolin has been identified to offer numerous health benefits, with preclinical studies highlighting its broad pharmacological potential, notably its antioxidant properties and capacity to scavenge reactive oxygen species (ROS) [10]. *In vivo* study involving mice has shown that luteolin effectively inhibits melanin synthesis, an effect attributed to the presence of additional hydroxyl groups on its B ring, specifically at the 3' carbon position. The structural nuances of flavonoid compounds, such as luteolin, are critical in determining their specific biological activities, with variations in structure influencing their efficacy in the melanogenesis pathway.

Further investigations into luteolin's effects have suggested its utility as a skin-whitening agent, attributable to its inhibitory action on tyrosinase activity and the α -MSH-mediated cAMP signaling pathway upstream. A notable study reported a significant increase (17.0-fold) in Agouti-signaling protein (ASIP) mRNA levels in human

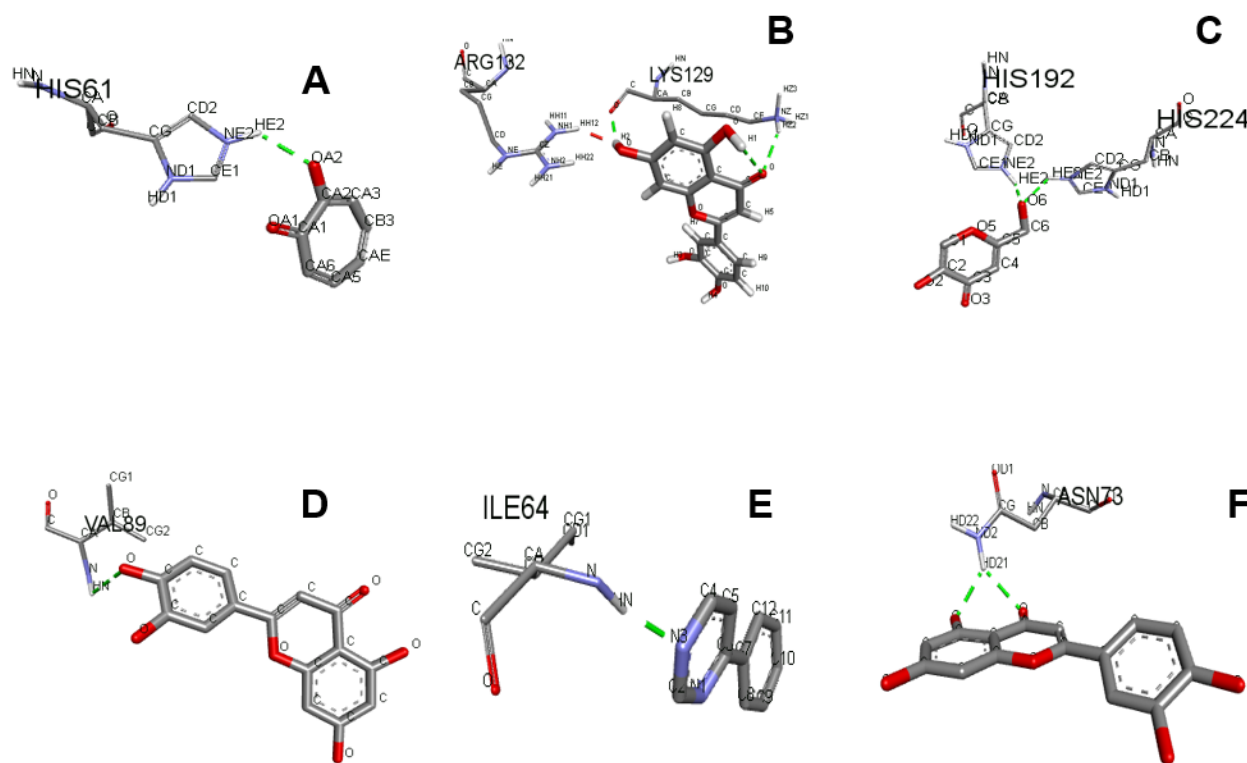


Figure 4. Visualization of native ligand and test compounds on target proteins. (A) Hydrogen bonding between tyrosinase target protein and native ligand OTR, (B) luteolin and, (C) Hydrogen binding between the target protein tyrosinase-related protein 1 and the native ligand KOJ, (D) luteolin, (E) hydrogen binding between the target protein of the enzyme D-dopachrome tautomerase and the native ligand RW1, (F) luteolin

A375 melanoma cells treated with luteolin [11]. ASIP acts as an antagonist to α -MSH, thereby inhibiting the melanin synthesis pathway [12]. Current understanding highlights the cAMP-PKA-MITF-tyrosinase schema in melanin synthesis, with the microphthalmia-associated transcription factor (MiTF) playing a pivotal role as the primary transcription factor. It activates not only tyrosinase but also dopachrome tautomerase and tyrosinase-related protein 1, in response to signals from melanocortin receptor 1 (MC1R). The anti-melanogenic effects of luteolin are predominantly mediated through its influence on the transcriptional factor MiTF and the melanogenesis enzymes—tyrosinase, dopachrome tautomerase, and tyrosinase-related protein 1 [13].

The optimization of the test compound (luteolin) was optimized using the AM1 semi-empirical method via the HyperChem8 software. This optimization involved a two-stage process: initially, a single-point calculation was performed, followed by geometry optimization. The results shown in Table 1 indicate that 3D structure optimization for luteolin has been successfully carried out because the lower energy of the compound can maximize its ability to donate

electrons; hence, the compound is more accessible to bind to the target protein. Low energy values also indicate interactions in the form of greater attraction between atoms. In contrast, the repulsive forces between atoms become minimal so that the compounds' conformation is more stable [14].

The preparation of the 3D structures of the target proteins—tyrosinase, tyrosinase-related protein 1, and D-dopachrome tautomerase—was aimed at separating these proteins from their native ligands. These selected proteins, comprising multiple chains, were initially bound to specific native ligands known for their inhibitory activities. For instance, the tyrosinase protein, with its four chains (A, B, C, and D), was bound to tropolone (OTR), a compound recognized for its tyrosinase inhibition properties [15]. Similarly, D-dopachrome tautomerase, consisting of three chains (A, B, and C), was associated with 4-phenyl pyrimidine (RW1), an inhibitor of the protein's activity. Lastly, tyrosinase-related protein 1, also with four chains (A, B, C, and D), was linked to 5-hydroxy-2-(hydroxymethyl)-4H-pyran-4-one (KOJ), a known inhibitor of this enzyme's activity [16].

For the molecular docking study, the selection of protein chains was specific: the B chain of tyrosinase with its native ligand tropolone (OTR), the A chain of tyrosinase-related protein 1 with the native ligand KOJ, and the C chain of D-dopachrome tautomerase with its native ligand 4-phenyl pyrimidine (RW1). We removed all non-selected chains and separated the native ligands from each target protein. Subsequently, we eliminated water molecules from the target proteins, following the detachment of native ligands. Figures 2 and 3 respectively illustrate the results of the target protein preparation and the structure of the target protein chain alongside its native ligand.

The validation of our docking method relied on the Root Mean Square Deviation (RMSD) value as a critical parameter. RMSD values gauge the similarity between the docked native ligands and their crystallographic positions on the protein, with lower RMSD values indicating a more accurate representation of the ligand's native conformation and binding site affinity. A docking method is considered valid if it achieves an RMSD value of ≤ 3 Å [9].

We then proceeded to configure the grid box, adjusting its size to encompass both the native ligand and the test compound, ensuring the native ligand was centrally positioned within the grid box. The grid box's dimensions (x, y, z) were tailored to create an optimal docking space, with its location on the protein macromolecule adjusted through the centers (x, y, z). It is noted that an increase in grid box size could potentially elevate the RMSD value [17]. Table 2 provides the grid size coordinates and the grid center in the target protein's grid box. The chosen conformations for tyrosinase, tyrosinase-related protein 1, and D-dopachrome tautomerase demonstrated RMSD values of 0.99 Å, 2.25 Å, and 2.42 Å, respectively.

From the docking study, the conformation exhibiting the lowest (most negative) bond energy was selected out of the top ten conformations. Specifically, conformation 9 was chosen for tyrosinase, conformation 2 for tyrosinase-related protein 1, and conformation 1 for D-dopachrome tautomerase. The interaction obtained shows hydrogen bond are formed. Table 3 presents the docking results, including interactions between the native ligands, the test compound (luteolin), and the target proteins. Notably, the docking of luteolin with each target protein resulted in the formation of hydrogen bonds, indicating interaction between the compound and the proteins. The results of the visualization of the

overall interaction between the test compound and each target protein are shown in Figure 4.

The bond energy values obtained from the docking of luteolin with the three target proteins were negative, signifying the affinity (or bond strength) between the test compound and the proteins [18]. A comparison of the bond energy outcomes, as detailed in Table 3, shows that the binding energy of luteolin is more negative than that of the native ligands. This implies a stronger and more stable affinity of luteolin as an inhibitor of the melanogenesis enzyme activity in the target proteins.

Furthermore, the analysis highlights the occurrence of hydrophobic interactions, which arise when nonpolar groups from a compound and a receptor are enveloped by water molecules [19]. These interactions underscore the diversity of bonds that can form in such molecular docking processes, including hydrogen, Van der Waals, hydrophobic, and electrostatic bonds.

In this study, the amino acid residues His61, Lys129, and Arg132 were identified as crucial for hydrogen bond formation between luteolin and the tyrosinase enzyme. This finding contrasts with an *in silico* study of 2-methoxyphenyl derivative compounds docked with tyrosinase, which implicated His61, His259, Pro277, Ser282, and Val283 in protein-ligand interactions. Notably, Val283, His263, and Phe264 are reported as major residues within the active site of tyrosinase, with additional active site residues including His244, Glu256, Asn260, and Ala286, among others [20]. The discrepancy in amino acid involvement suggests variations in ligand binding due to differences in physicochemical properties such as size, shape, charge, polarity, and hydrophobicity. These variations influence the nature of interactions, including electrostatic interactions, hydrogen bonds, Van der Waals forces, and hydrophobic interactions, thereby affecting the compound's inhibitory potential on tyrosinase.

For tyrosinase-related protein 1, the amino acid residues His192, His224, and Val89 were involved in hydrogen bond formation with luteolin. Tyrosinase-related protein 1 is structured into four domains, with amino acid residues such as Arg374, His377, His381, His404, Ser394, His224, His215, His192, Thr391, and Tyr362 situated on the active site and interacting directly with substrates [21]. This delineation implies that luteolin's interaction involves active site residues of tyrosinase-related protein 1, indicating potential inhibitory activity.

With D-dopachrome tautomerase, the residues Ile64 and Asn73 participated in forming hydrogen bonds with luteolin, underscoring the specificity of luteolin's interaction with different melanogenesis enzymes.

These findings suggest luteolin's potential as an antihyperpigmentation agent, evidenced by its inhibitory interactions with the active sites of melanogenesis enzymes—tyrosinase, tyrosinase-related protein 1, and D-dopachrome tautomerase. This *in silico* study serves as a preliminary assessment, predicting the ligand-receptor interactions and highlighting luteolin's capacity to inhibit melanin synthesis. However, to validate luteolin's efficacy, further *in vitro* and *in vivo* studies are recommended.

Conclusion

Luteolin demonstrates a notable affinity for the target proteins associated with melanogenesis—tyrosinase, tyrosinase-related protein 1, and D-dopachrome tautomerase—as evidenced by the negative bond energy values obtained from docking studies. Notably, the bond energy values for luteolin with each of these target proteins are more negative than those for their respective native ligands, indicating a stronger affinity. The interactions between luteolin and the target proteins involve various types of bonds, including hydrogen, Van der Waals, hydrophobic, and electrostatic bonds. Specifically, the amino acid residues His61, Lys129, and Arg132 are implicated in the formation of hydrogen bonds in the interactions between luteolin and tyrosinase. In the case of tyrosinase-related protein 1, the residues His192, His224, and Val89 are involved in hydrogen bonding. For D-dopachrome tautomerase, Ile64 and Asn73 participate in forming hydrogen bonds with luteolin.

These docking results underscore luteolin's potential as an effective antihyperpigmentation agent, primarily through its inhibitory action on enzymes crucial for melanin synthesis. The specificity and strength of its interactions with these melanogenesis enzymes suggest that luteolin could serve as a potential inhibitor, providing a foundation for further research into its application in treating hyperpigmentation.

Acknowledgment

We would like to take this opportunity to thank you Department of Pharmacy and Faculty of Mathematics

and Natural Sciences for providing the facilities used in this research.

Declaration of interest

The authors declare no conflict of interest.

Author contributions

LALNP conceptualized the study design, NLAKE wrote the original draft, LALNP, NLAKE, NPLL, and NMPS reviewed and edited the final person. NPLL and NMPS supervised all experiments. All authors have read the final manuscript.

Received: August 14, 2023

Revised: February 2, 2024

Accepted: February 12, 2024

Published online: March 31, 2024

References

1. Brettmann EA, de Guzman Strong C. Recent evolution of the human skin barrier. *Exp Dermatol*. 2018;27: 859–866. <https://doi.org/10.1111/exd.13689>
2. El Howati A, Tappuni A. Systematic review of the changing pattern of the oral manifestations of HIV. *J Investig Clin Dent*. 2018;9: e12351. <https://doi.org/10.1111/jicd.12351>
3. Pulungan A, Soesanti F, Tridjaja B, Batubara J. Vitamin D insufficiency and its contributing factors in primary school-aged children in Indonesia, a sun-rich country. *Ann Pediatr Endocrinol Metab*. 2021;26: 92–98. <https://doi.org/10.6065/apem.2040132.066>
4. Pérez-Bernal A, Muñoz-Pérez MA, Camacho F. Management of facial hyperpigmentation. *Am J Clin Dermatol*. 2000;1: 261–268. <https://doi.org/10.1111/pcmr.12986>
5. Kollias N, Sayre RM, Zeise L, Chedekel MR. New trends in photobiology: Photoprotection by melanin. *J Photochem Photobiol B*. 1991;9: 135–160. [https://doi.org/10.1016/1011-1344\(91\)80147-A](https://doi.org/10.1016/1011-1344(91)80147-A)
6. Briganti S, Picardo M. Antioxidant activity, lipid peroxidation and skin diseases. What's new. *J Eur Acad Dermatol Venereol*. 2003;17: 663–669. <https://doi.org/10.1046/j.1468-3083.2003.00751.x>
7. Arifin B, Ibrahim S. Struktur, Bioaktivitas dan Antioksidan Flavonoid. *Jurnal Zarah*. 2018;6: 21–29. <https://doi.org/10.31629/zarah.v6i1.313>
8. Lee SW, Kim JH, Song H, Seok JK, Hong SS, Boo YC. Luteolin 7-Sulfate Attenuates Melanin Synthesis through Inhibition of CREB- and MITF-Mediated Tyrosinase Expression. *Antioxidants*. 2019;8. <https://doi.org/10.3390/antiox8040087>
9. Jain AN, Nicholls A. Recommendations for evaluation of computational methods. *J Comput Aided Mol Des*. 2008;22: 133–139. <https://doi.org/10.1007/S10822-008-9196-5>

10. Taheri Y, Sharifi-Rad J, Antika G, Berkay Yilmaz Y, Tumer TB, Abuhamdah S, et al. Review Article Paving Luteolin Therapeutic Potentialities and Agro-Food-Pharma Applications: Emphasis on In Vivo Pharmacological Effects and Bioavailability Traits. *Hindawi Oxidative Medicine and Cellular Longevity*. 1987;2021: 20. <https://doi.org/10.1155/2021/1987588>
11. Choi MY, Song HS, Hur HS, Sim SS. Whitening activity of luteolin related to the inhibition of cAMP pathway in alpha-MSH-stimulated B16 melanoma cells. *Arch Pharm Res*. 2008;31: 1166–1171. <https://doi.org/10.1007/S12272-001-1284-4>
12. Suzuki I, Tada A, Ollmann MM, Barsh GS, Im S, Lamoreux ML, et al. Agouti signaling protein inhibits melanogenesis and the response of human melanocytes to alpha-melanotropin. *J Invest Dermatol*. 1997;108: 838–842. <https://doi.org/10.1111/1523-1747.ep12292572>
13. Liu-Smith F, Meyskens FL. Molecular mechanisms of flavonoids in melanin synthesis and the potential for the prevention and treatment of melanoma. *Mol Nutr Food Res*. 2016;60: 1264. <https://doi.org/10.1002/MNFR.201500822>
14. Hypercube. Hyperchem Release 7: Tools for Molecular Modelling. 2002. Hypercube Incorporation, Canada.
15. Ismaya WT, Rozeboom HJ, Weijn A, Mes JJ, Fusetti F, Wichers HJ, et al. Crystal structure of agaricus bisporus mushroom tyrosinase: Identity of the tetramer subunits and interaction with tropolone. *Biochemistry*. 2011;50: 5477–5486. <https://doi.org/10.1021/bi200395t>
16. Lai X, Wichers HJ, Soler-Lopez M, Dijkstra BW. Structure of Human Tyrosinase Related Protein 1 Reveals a Binuclear Zinc Active Site Important for Melanogenesis. *Angewandte Chemie International Edition*. 2017;56: 9812–9815. <https://doi.org/10.1002/anie.201704616>
17. Feinstein WP, Brylinski M. Calculating an optimal box size for ligand docking and virtual screening against experimental and predicted binding pockets. *J Cheminform*. 2015;7: 1–10. <http://dx.doi.org/10.1186/s13321-015-0067-5>
18. Mukesh B, Rakesh K. Molecular Docking: a Review. *Int J Res Ayurveda Pharm*. 2011;2: 1746–1751. Available: www.ijrap.net
19. Kong R, Yang G, Xue R, Liu M, Wang F, Hu J, et al. COVID-19 Docking Server: a meta server for docking small molecules, peptides and antibodies against potential targets of COVID-19. *Bioinformatics*. 2020;36: 5109–5111. <https://doi.org/10.1093/bioinformatics/btaa645>
20. Zargasam MK, Ahmed M, Akhtar N, Ashraf Z, Maksoud MAA, Aufy M, et al. Synthesis, In Silico Studies, and Antioxidant and Tyrosinase Inhibitory Potential of 2-(Substituted Phenyl) Thiazolidine-4-Carboxamide Derivatives | Enhanced Reader. In: *Pharmaceuticals*. 2023 pp. 1–15. <https://doi.org/10.3390/ph16060835>
21. Puspita PJ, Liliyani NPP, Ambarsari Laksmi. In Silico Analysis of Active Compounds of Avocado Fruit (*Persea americana* Mill.) as Tyrosinase Enzyme Inhibitors. *Current Biochemistry*. 2022;9: 73–87. <https://doi.org/10.29244/cb.9.2.3>